

# Lawrence Berkeley National Laboratory

## Recent Work

### Title

HIGH RESOLUTION SPECTROMETRY FOR RELATIVISTIC HEAVY IONS

### Permalink

<https://escholarship.org/uc/item/3fd3b0fn>

### Author

Gabor, G.

### Publication Date

1975-05-01

Submitted to Nuclear Instruments  
and Methods

LBL-3833  
Preprint 9 /

HIGH RESOLUTION SPECTROMETRY FOR  
RELATIVISTIC HEAVY IONS

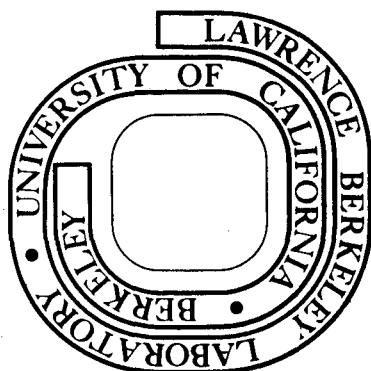
G. Gabor, W. Schimmerling, D. Greiner  
F. Bieser and P. Lindstrom

May 1975

Prepared for the U. S. Energy Research and  
Development Administration under Contract W-7405-ENG-48

**For Reference**

Not to be taken from this room



LBL-3833  
9 /

## **DISCLAIMER**

This document was prepared as an account of work sponsored by the United States Government. While this document is believed to contain correct information, neither the United States Government nor any agency thereof, nor the Regents of the University of California, nor any of their employees, makes any warranty, express or implied, or assumes any legal responsibility for the accuracy, completeness, or usefulness of any information, apparatus, product, or process disclosed, or represents that its use would not infringe privately owned rights. Reference herein to any specific commercial product, process, or service by its trade name, trademark, manufacturer, or otherwise, does not necessarily constitute or imply its endorsement, recommendation, or favoring by the United States Government or any agency thereof, or the Regents of the University of California. The views and opinions of authors expressed herein do not necessarily state or reflect those of the United States Government or any agency thereof or the Regents of the University of California.

## HIGH RESOLUTION SPECTROMETRY FOR RELATIVISTIC HEAVY IONS\*

G. Gabor, W. Schimmerling, D. Greiner  
F. Bieser and P. Lindstrom

Lawrence Berkeley Laboratory  
University of California  
Berkeley, California 94720 U.S.A.

ABSTRACT

Several techniques are discussed for velocity and energy spectrometry of relativistic heavy ions with good resolution. A foil telescope with chevron channel plate detectors is described. A test of this telescope was performed using 2.1 GeV/A  $C^{6+}$  ions, and a time-of-flight resolution of 160 ps was measured. Qualitative information on the effect of foil thickness was also obtained.

---

\* This work was performed under the auspices of the United States Energy Research and Development Administration.

## 1. INTRODUCTION

The recent availability of relativistic heavy ion beams has brought about the need for adequate spectrometry. Typical experiments involve particle identification, isotope separation and accurate energy loss measurements. The resolutions (FWHM) desired are approximately 0.1% energy or 100 ps time of flight (TOF). Velocity measurements are not directly equivalent to energy or momentum measurements unless the mass (or charge) of the heavy ion is also known. Velocity measurements, however, are in addition easily related to absolute standards. Some experiments require that a minimum amount of material be interposed in the beam. The need for a heavy ion spectrometer that introduces a minimum of material into the beam suggests the use of transmission detectors or magnet spectrometers. The transmission detectors can be used as direct  $dE/dx$  detectors or as components of a time-of-flight telescope.

We review several techniques to satisfy these requirements. The optimum detector for several types of experiments is a foil telescope with channel plate detectors. An experimental test of such a telescope is described and it is shown that a TOF resolution of 160 ps can be obtained.

### A. Magnet Spectrometers

Magnet spectrometers can be used in conjunction with multiwire proportional counters (MWPC) to measure the momentum of a particle by defining its trajectory through a magnet. Two particles with momenta  $P$  and  $P + \Delta P$  will arrive at the detector with a certain separation. This separation must be greater than the beam spot size if they are to be resolved. The angular displacement is  $\Delta\theta = d/L$ , where  $d$  is the beam spot diameter and  $L$  is the distance between the magnet and the detector plane. The required relative angular resolution,  $\Delta\theta/\theta = \Delta P/P$ , is 0.1%. For a beam spot of 1 cm diameter, this is equivalent to requiring  $L \cdot \theta \geq 10^3$  (rad·cm) to  $L \cdot \theta \geq 573$  (deg·m). Practical magnets have bending powers of the order to 1400 to 3000 KG·cm. For a 1 GeV/A beam of particles having a mass to charge ratio

of 2, the maximum bending angle is about  $15^\circ$ . Thus, a drift length of 30 to 40 m is necessary for a single magnet to separate the particles at the detector.

The energy of a heavy ion before and after it traverses an absorber can thus be measured with the required resolution using a magnet spectrometer. However, the full momentum range desired can only be covered using very strong magnetic fields (or multiple magnets) and very long beam lines. The disadvantages of this approach are its high cost and problems due to magnetic field shapes, which have not been discussed.

#### B. Scintillators

The pulse-height resolution of scintillators is a few percent<sup>1)</sup>. In addition, their light output saturates as a function of  $dE/dx$  below  $\sim 100 \text{ MeV/A}$ <sup>2)</sup>. This limits their use in direct measurements of stopping power. However, scintillators are inexpensive, easy to use and produce very fast signals. These qualities make it desirable to consider the use of thin scintillators.

A reasonable scintillator thickness to minimize background and energy straggling is  $50 \text{ mg/cm}^2$  (500 microns thick). The total energy deposited is  $\approx 1 \text{ MeV}$ . To find the time resolution, the overall 'detector' timing characteristics have to be considered. A scintillation detector consists of a scintillator, a coupling device and a photomultiplier with a gain of  $10^7$ . The time resolution of this detector depends mainly on the number of photoelectrons produced at the photomultiplier. This number is severely limited by the small solid angle subtended by the thin scintillator. The best resolution that can be expected, including the time dispersion in the photomultiplier, is  $\sim 300 \text{ ps}$ <sup>3)</sup>.

### C. Use Of Thin Silicon $\Delta E$ Detectors

Semiconductor detectors are more efficient than plastic scintillators ( $\epsilon \sim 3.7$  eV/electron hole pair<sup>4</sup>) and therefore provide an inherently better signal-to-noise ratio than the latter. The thickness of the detector is also constrained by the variation in  $dE/dx$ . It must be  $\sim 100$   $\mu\text{m}$  for an energy loss  $< 0.1\%$ . The energy deposited,  $\sim 1$  MeV, is such that the energy resolution is dominated by the electronic noise. As shown in Ref. 4, the expected energy resolution is 10 to 20 keV, or 1 to 2%. The same considerations regarding straggling apply here as before.

Measurements of  $\Delta E$  of highly charged heavy ions at these energies are also affected by the loss of high energy delta rays and by nuclear interactions<sup>5</sup>).

Large areas are convenient in experiments but thin large active area detectors (above  $\sim 7$  mm x 5 mm) are difficult to fabricate. The use of thin detectors results in a large capacitance and small energy deposition. This degrades the signal-to-noise ratio and increases the timing dispersion according to:<sup>4</sup>)

$$\Delta t_n = (4C/\Delta E) (\tau/g_m)^{1/2} \quad (1)$$

where  $C = C_D + C_{\text{FET}}$  is the total input circuit capacitance,  $C_{\text{FET}}$  is the gate capacitance of the FET commonly used in the preamplifier input.  $C_D = 1.05 A/T$  is the detector capacitance,  $A$  is the total active detector area,  $\Delta E$  is the energy deposited in the detector,  $T$  is the thickness,  $\tau$  is the risetime at the preamplifier input ( $\sim 1$  ns), and  $g_m$  is the transconductance of the FET ( $\sim 50$  mA/V).

The overall time resolution  $\Delta t$  is given by:

$$(\Delta t)^2 = (\Delta t_E)^2 + (\Delta t_n)^2 \quad (2)$$

where  $\Delta t_E$  is the contribution due to the dispersion mechanisms of the charge collection.

In thick detectors, the contribution of  $\Delta t_E$  predominates due to the increase in electron collection time, which produces a slower risetime and consequently a poorer time pick-off signal.

Inhomogeneities in the field gradient through the bulk of the detector will cause additional dispersion. Using time resolutions measured at our laboratory for 8.75 MeV alpha particles, we compute the time resolution to be expected for 2.1 GeV/A carbon ions as 700 ps for a 20  $\mu\text{m}$  Si-detector and 400 ps for a 100  $\mu\text{m}$  Si-detector.

Thick silicon detectors have been used for total energy measurements at lower energies (Ref. 4). At relativistic energies the range is 10 to 100  $\text{gm/cm}^2$ , or 5 to 50 cm of silicon. Such an arrangement is impractical for obvious reasons (e.g. range straggling, change in effective  $\epsilon$  at end of range, fabrication differences, etc.).

Consideration also has to be given to radiation damage. Damage can occur either from the direct beam or the neutrons generated in a collimator. Damage begins to be noticed after a total energy deposition (dose) of  $\sim 10^9$  rads<sup>6</sup>). It is also dependent upon the stopping power. Damage is usually seen as an increase in leakage current which predictably degrades the energy and timing resolution.

#### D. Foil TOF Telescopes

The thin foil cathode detector (TFCD) utilizing a chevron channel plate multiplier (CCPM)\* was developed at LBL to measure the energy of 1 to 8 MeV/A heavy ions produced at the Super Hilac. The goal during the development of the detector was to produce the lowest time jitter possible. For this reason, the electron optics used in the TFCD are parallel plane to eliminate electron flight path variations due to focusing.

A standard channel plate multiplier (CPM) is made by cutting a slice out of a bundle of lead glass capillary tubes fused together and drawn to achieve the right diameter (10 to 50  $\mu\text{m}$ ). In this configuration the surface of the channel plate is

---

\* Purchased from Galileo Electro-optics Corporation, Galileo Park, Sturbridge, Massachusetts 01518, U.S.A.



perpendicular to the capillary axis. The plate is then exposed to a chemically reducing atmosphere to produce slightly conductive channel walls ( $10^{10}$  to  $10^{12} \Omega$  per channel). The resistive surface of the channel walls forms a continuous divider-dynode electron multiplier.

The gain achievable with a single plate is limited by positive ion feedback. The ions are formed at the output of a channel where a dense electron cloud is produced when input electrons are multiplied. The residual gas is ionized and the positive ions are accelerated toward the input end of the channel where they produce more electrons from the walls. The resulting electrons are multiplied again. This feedback can saturate the multiplier as shown in Fig. 1.

Positive ion feedback can be eliminated by using a plate with channels cut at a bias angle ( $8^\circ$  to  $15^\circ$ ) together with a standard plate as shown in Fig. 2. The positive ions produced at the output of the standard plate cannot reach the input of the bias plate. Both plates are operated at a gain of  $\sim 10^3$ . This gain is well below the limit where positive ion feedback becomes significant. Thus, the positive ions are restricted to a section of gain  $10^3$ , while the signal is amplified in both plates with an overall gain of  $10^6$ .

The TFCD (Fig. 3) consists of a foil in which electrons are produced by the incident charged particles. Electrons of energies typically below 2 eV are accelerated into a field-free region and impinge on the channels of the CCPM. After multiplication in the CCPM, the electrons are collected by a  $50 \Omega$  coaxial anode.

The detector has inherently good time resolution. The only mechanisms for time dispersion are the multiplication process and the geometrical dispersion. The latter is easily eliminated. The intrinsic time dispersion due to channel multiplication can be estimated to be less than 75 ps.

The use of thin foils allows a minimum of material to interact with the beam. The minimum thickness of the foils is constrained by the number of electrons produced with energies  $< 2$  eV. The optimum foil thickness corresponds to the maximum of electron buildup. In practice, foils of  $20 \mu\text{g}/\text{cm}^2$  to  $1 \text{mg}/\text{cm}^2$  have been found adequate.

## 2. EXPERIMENTAL ARRANGEMENT

A brief test was carried out in the Bevatron heavy ion calibration facility<sup>7)</sup>. A beam of 2.1 GeV/A C<sup>6+</sup> ions was used. The beam was collimated by a 1.3-cm diameter aperture ~ 20 m upstream of the detectors. The detector arrangement is shown schematically in Fig. 4.

The beam was incident on two MWPCs  $W_1$  and  $W_2$ , which were used to monitor beam spot size and position throughout the run. The beam then traversed a 0.6 x 0.6 x 0.3 cm scintillator  $S_1$ , the ~8 mm diameter foils in channel plate detectors  $CP_1$  and  $CP_2$ , an ~8 mm diameter, 130  $\mu$ m thick surface barrier silicon semiconductor detector SS, a scintillator  $S_2$  identical to  $S_1$ , and a particle identification telescope T<sup>8)</sup>. The channel plate detectors and SS were housed in a vacuum chamber at  $\sim 2 \times 10^{-6}$  Torr. A 2.5 cm thick brass flange covered the entrance port and a 1.25 cm thick aluminum flange covered the exit port. The flight path, defined by the separation of the  $CP_1$  and  $CP_2$  foils, was 40 cm.

The apparatus was initially aligned optically. The alignment was refined at the start of the run by optimizing the efficiency, defined by the count rate in SS, and then the event rate, relative to the counting rate in T. It became evident at this time that perfect beam alignment would be difficult to achieve due to the small size of the detectors. The off-axis position of the collimator further limited our beam steering possibilities. We concluded that for the purpose of this test, the misalignment was tolerable. An efficiency of approximately 1% was accepted because of the limited beam time available for this test.

## 3. EXPERIMENTAL ELECTRONICS

Signals from the following detectors, shown in Fig. 4, were used:

- 1) Two wire chambers,  $W_1$  and  $W_2$  each of which provided X and Y position information for every incident particle.

- 2) Two plastic scintillators,  $S_1$  and  $S_2$ , intended to define the trajectory of particles through the foil telescopes.
- 3) The foil telescope  $CP_1$  and  $CP_2$ , consisting of two foils at  $45^\circ$  to the beam path, each viewed by a CCPM with its own fast pre-amplifier, main amplifier and constant fraction discriminator.
- 4) The silicon detector, SS, aligned with the telescope.
- 5) The four-segment silicon detector particle identifier,<sup>8)</sup> T, which provided information on those beam particles not interacting in the intervening material.

The electronics for the detectors mentioned in 1), 2) and 5) have been described elsewhere<sup>7, 8)</sup> and that for SS is standard<sup>4)</sup>. Only the electronics for the foil telescope are discussed here. Figure 5 shows the circuit schematic for the TOF telescope.

The TOF of the particles was measured using a time-to-amplitude converter (TAC). The START signal was obtained from  $CP_1$  and the STOP signal from  $CP_2$ . In addition, the TAC was gated by SS.

The TAC output, the amplitude of the SS signal and 5% of the amplitude of the signal in  $CP_1$ , were each digitized in computer-controlled analog-to-digital converters (ADC). The strobe was provided by the T detector. For each event, the beam position, as defined by the X, Y coordinates of  $W_1$  and  $W_2$ , the pulse heights in  $CP_1$  and SS, and the TOF were recorded on-line by the facility's PDP-11/20 computer. During data processing a coincident signal was required from  $W_1$ ,  $W_2$ ,  $CP_1$ ,  $CP_2$  and T to define an event. In addition, a coincident signal from one or both of  $S_1$  and  $S_2$  was required for some of the runs to define the apparatus alignment.

To preserve the advantage of the fast rise time of the CCPM, a fast amplifier-discriminator system developed at LBL was used. The preamplifier is a very low-noise X10, 800 ps rise time amplifier. The main amplifier is a X5, 800 ps rise time, 5 V output device. The discriminator is a constant fraction discriminator<sup>9)</sup>.

#### 4. CALIBRATION

The system time resolution, using a pulser at a fixed amplitude to measure the contribution due to noise, was 30 ps. The resolution for a 100:1 dynamic range was  $88 \pm 20$  ps for one discriminator and  $108 \pm 20$  ps for the other one. The total discriminator contribution to the TOF resolution thus was  $140 \pm 28$  ps.

The TOF system was checked using a  $^{212}\text{Po}$ - $^{212}\text{Bi}$  source with alpha particle energies of 6.0 and 8.78 MeV. The time resolution with these particles was  $150 \pm 10$  ps (Fig. 6).

#### 5. TOP RESULTS

The quantity of interest in this test was the relative TOF resolution and no absolute energy measurements were made. The TOF spectra were obtained for several values of the delay between the START and STOP signals. This delay was varied by introducing calibrated lengths of signal cable. A typical TOF spectrum in the linear region is shown in Fig. 7. The unshaded histogram has been obtained without imposing any cuts on the data other than a threshold requirement on the ADC to eliminate noise effects. The data have also been binned into 5-channel bins, to smooth statistical fluctuations, and normalized to the peak height. The shaded histogram was obtained by accepting only events corresponding to particles incident within  $\sim 5$  mm of the beam axis in  $W_1$  and  $W_2$ , requiring that particles registered in T have charge 6, and selecting events with a pulse height in SS corresponding to carbon. It may be seen that, while these cuts on the data reduce the tails of the TOF spectrum, the peak position remains unchanged.

The TOF measurements had several sources of error, which were not fully investigated. The apparatus misalignment resulted in very poor statistics. The interactions of the beam in the vacuum chamber flanges resulted in scattered particles that were detected by some of the detectors but not in others, and caused a significant number of spurious events. However, peak position is a property of the total number of events, and was determined as a centroid. Systematic effects were explored by looking at various subsets of the data.

These cuts reduced the number of events (by a factor of  $\sim 6$  due to the poor experimental geometry) but had no effect on peak position. We therefore feel confident that the TOF resolution was not affected.

A plot of TOF peak channel position vs. time delay  $\Delta t$  is shown in Fig. 8. The slope of the linear region corresponds to 6.5 ps/channel. The non-linearity at small  $\Delta t$  was introduced by the TAC. All resolution data were measured with  $\Delta t \sim 24$  ns. The shape of the TOF spectrum did not change for  $16 \text{ ns} \leq \Delta t \leq 24 \text{ ns}$ . The spectra taken all fell within 25 channels (or  $\sim 160$  ps). If this is taken as the full width at half-maximum, the corresponding standard deviation is  $\sim 70$  ps. The energy of the beam in the flight path can be estimated at  $\sim 800$  MeV/A, corresponding to a TOF of  $\sim 160$  ns, and a TOF resolution of 0.1%.

## 7. CONCLUSIONS

The foil telescope seems to satisfy the requirements for a high-resolution TOF spectrometer for high-energy heavy ions. It compares favorably with other systems we have considered. We have achieved 160 ps resolution. This should be considered as an upper limit to the attainable resolution, which may be as low as  $\sim 100$  ps.

Several foil thicknesses were also tried although only qualitative information could be obtained. We found that a  $1 \text{ mg/cm}^2$  thick Pt foil resulted in a signal equivalent to  $\sim 4$  electrons per beam particle. A  $20 \text{ } \mu\text{g/cm}^2$  thick C foil, by comparison, gave a signal equivalent to less than one electron for every five beam particles.

We would like to thank Clark Hartsock for his assistance in the setting-up and babysitting of this equipment.

REFERENCES

- 1) W. R. Webber and J. Kish, Nucl. Instr. and Meth. 99 (1972) 237.
- 2) G. D. Badhwar, C. L. Deney, B. R. Dennis, and M. F. Kaplon, Nucl. Instr. and Meth. 57 (1967) 116.
- 3) B. Leskovar and C. C. Lo, IEEE Trans. Nucl. Sci. NS-19 (1972) 50.
- 4) Fred S. Goulding and Donald A. Landis, "Semiconductor Detector Spectrometer Electronics", Chp. III. D, Part A in Nuclear Spectroscopy and Reactions, J. Cerny Editor, Academic Press (1974) 414.
- 5) H. D. Maccabee, Radiation Res. 54 (1973) 495.
- 6) G. Dearnaley and D. C. Northrop, Semiconductor Counters for Nuclear Radiations, John Wiley, Inc., New York (1963) Chp. 10, 265.
- 7) D. E. Greiner, P. J. Lindstrom, F. S. Bieser and H. H. Heckman, Nucl. Instr. and Meth. 116 (1974) 21.
- 8) D. E. Greiner, Nucl. Instr. and Meth. 103 (1972) 291.
- 9) C. C. Lo and B. Leskovar, IEEE Trans. Nucl. Sci. NS-21 (1974) 93.

FIGURE CAPTIONS

- Fig. 1 Positive ion feedback for a chevron and a single-channel plate multiplier array.
- Fig. 2 Schematic of the positive ion feedback process.
- Fig. 3 Thin-foil cathode detector.
- Fig. 4 Schematic of experimental arrangement.
- Fig. 5 Electronics for TOF telescope.
- Fig. 6 TOF spectrum for the  $^{212}\text{Po} - ^{212}\text{Bi}$  alpha particle source used for calibration.
- Fig. 7 TOF spectrum for the 2.1 GeV/A  $\text{C}^{6+}$  heavy ion beam. The data have been binned into 5 channel bins and normalized for equal peak height. The shaded histogram corresponds to events selected by cuts in the data as described in the text ( $\sim 260$  events). It is contained within 160 ps. The unshaded histogram corresponds to all events satisfying the trigger logic ( 1600 events).
- Fig. 8 TOF spectrum peak channel as a function of time delay  $\Delta t$ . TOF resolution was measured with  $\Delta t = 24$  ns.

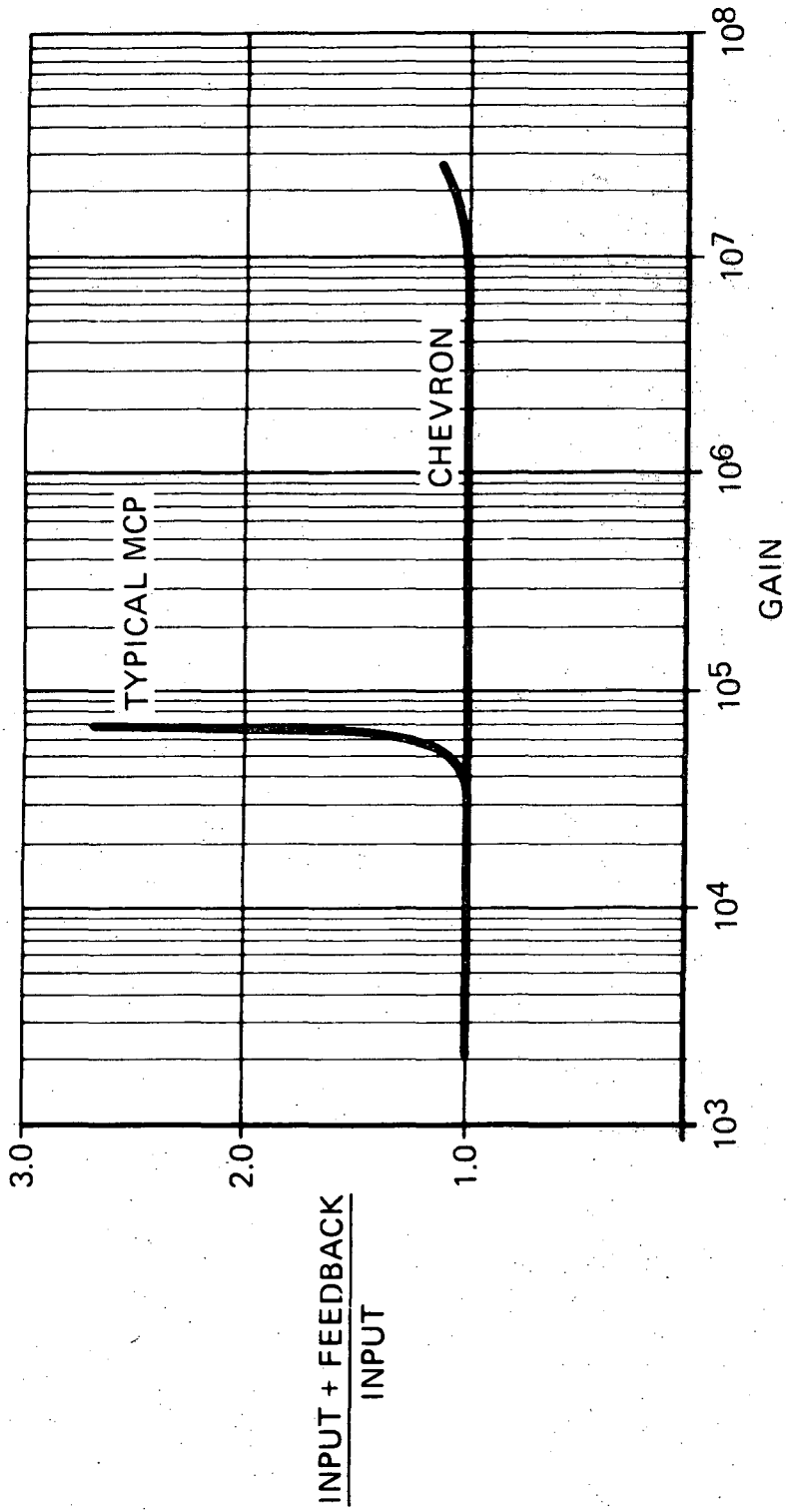


Fig. 1

XBL 743-590



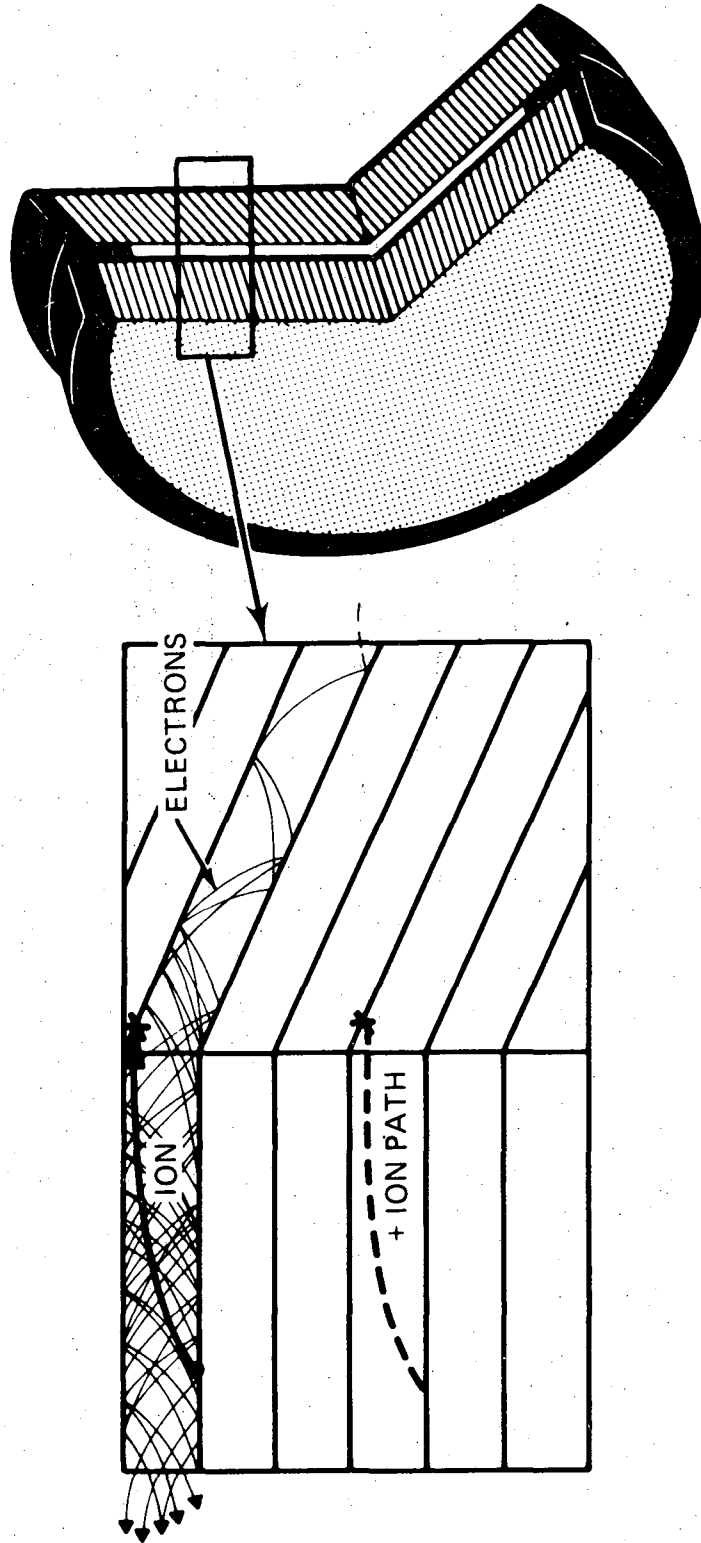


Fig. 2

XBL 743-589

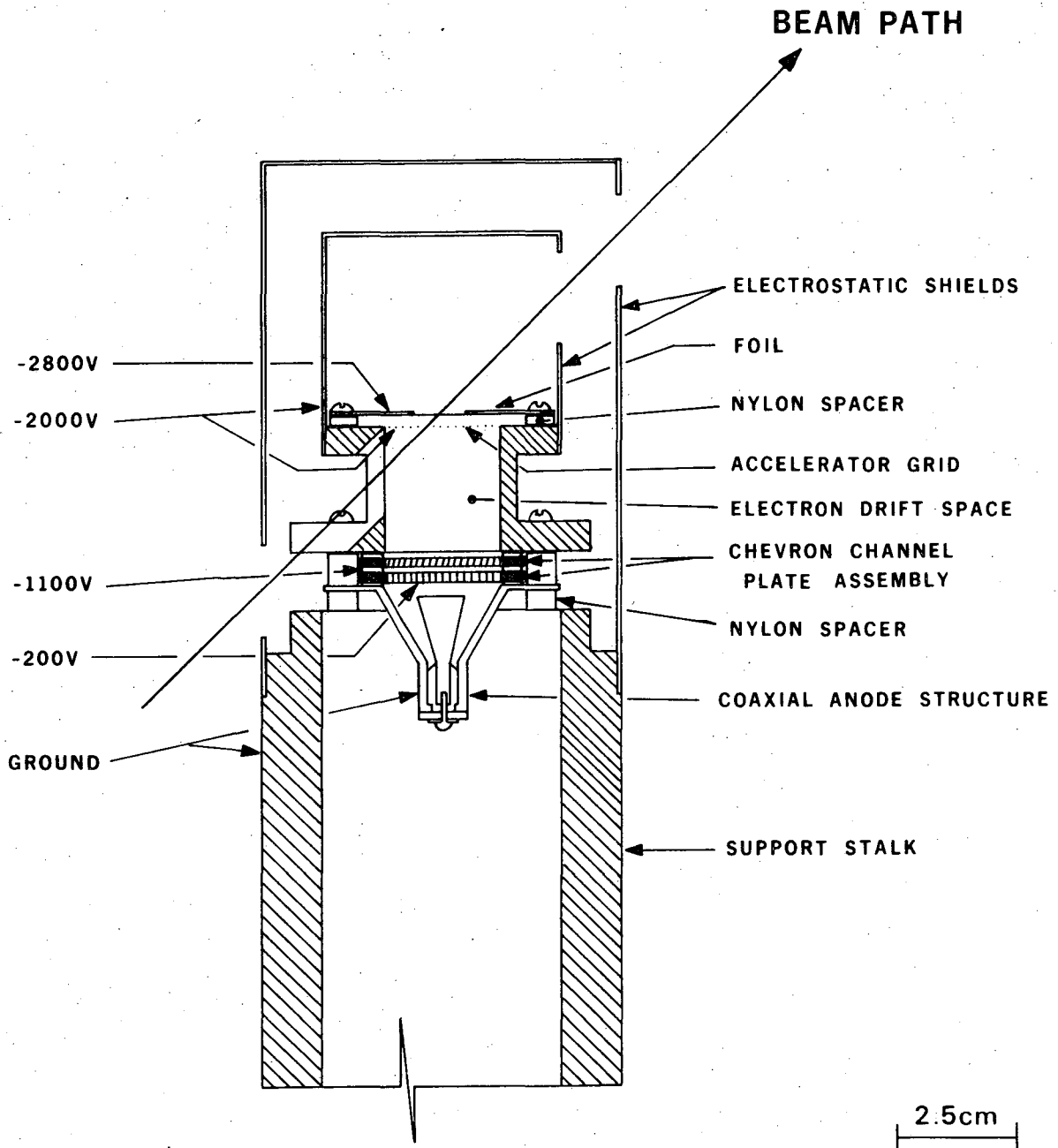
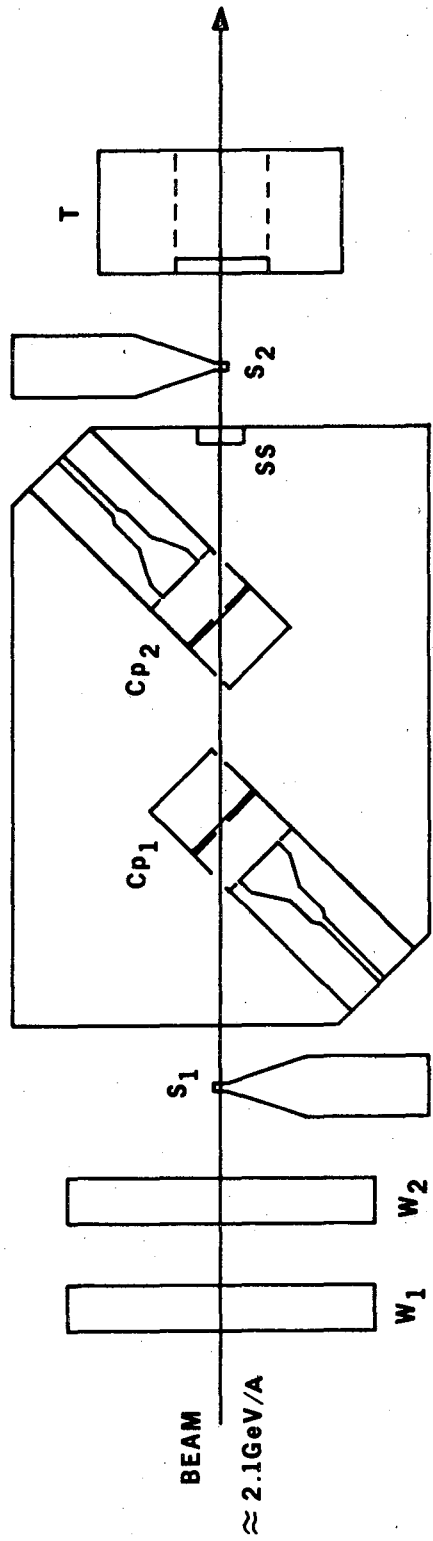


Fig. 3

XBL755-4897



XBL755-4898

Fig. 4

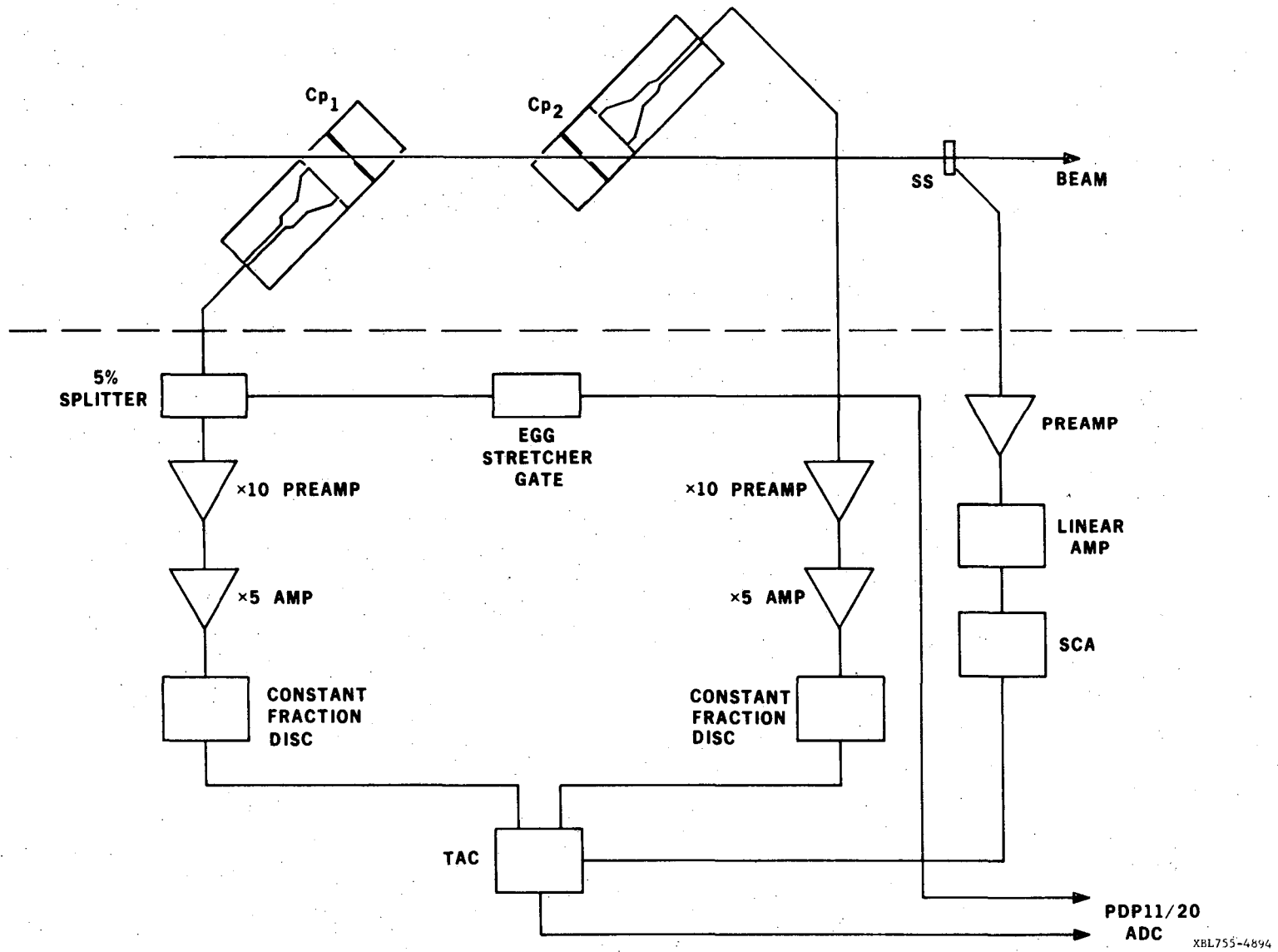
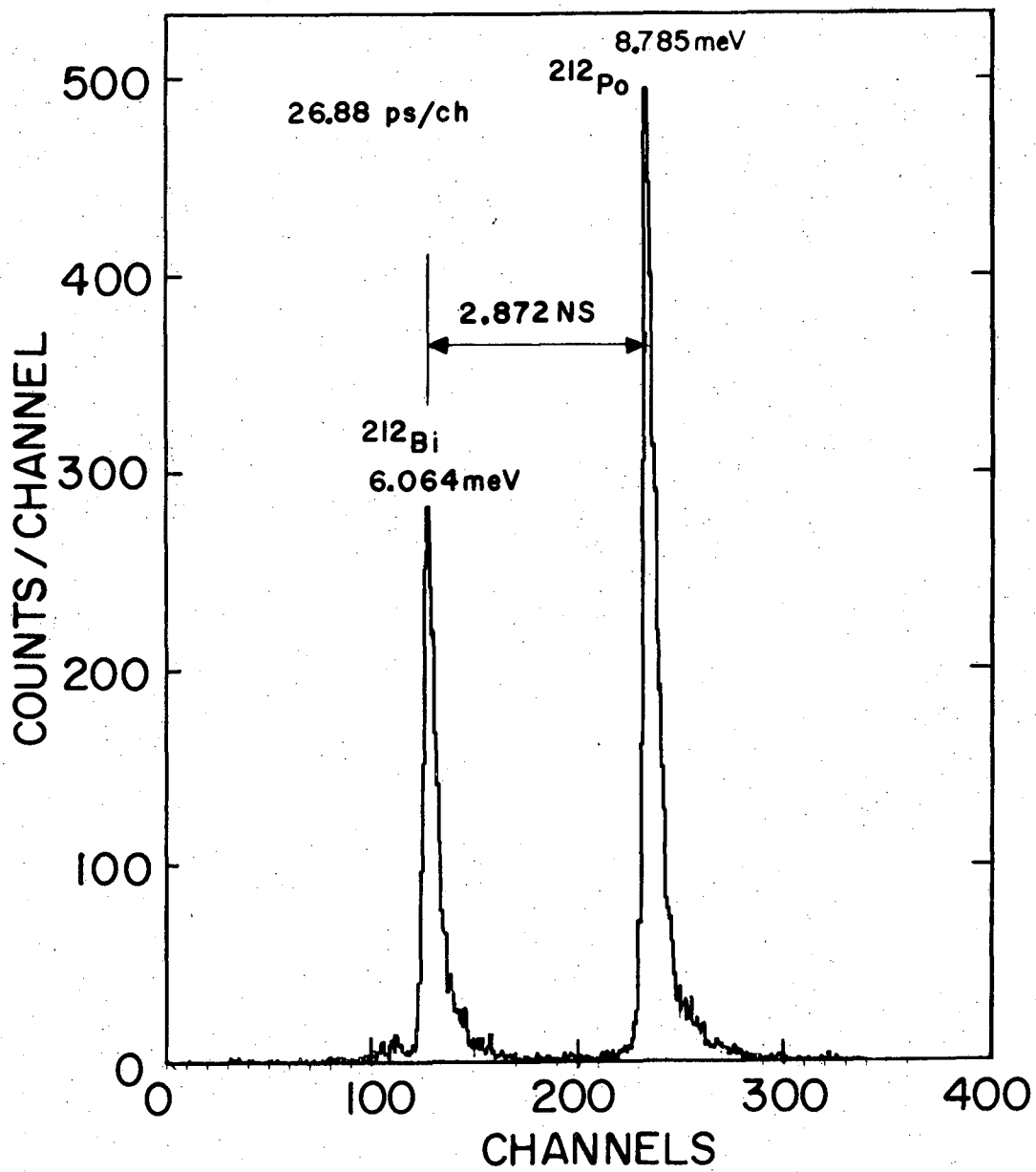
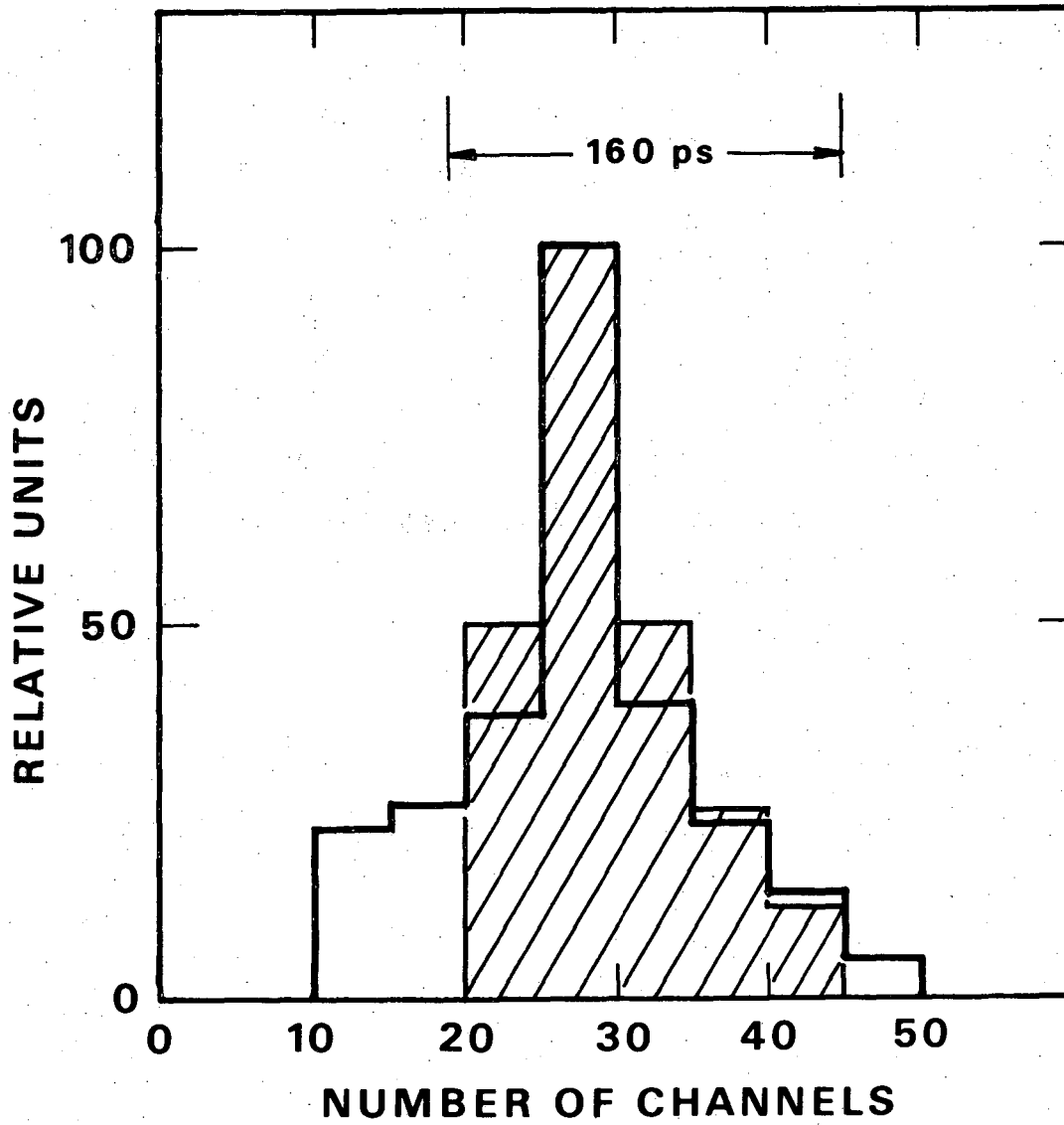


Fig. 5



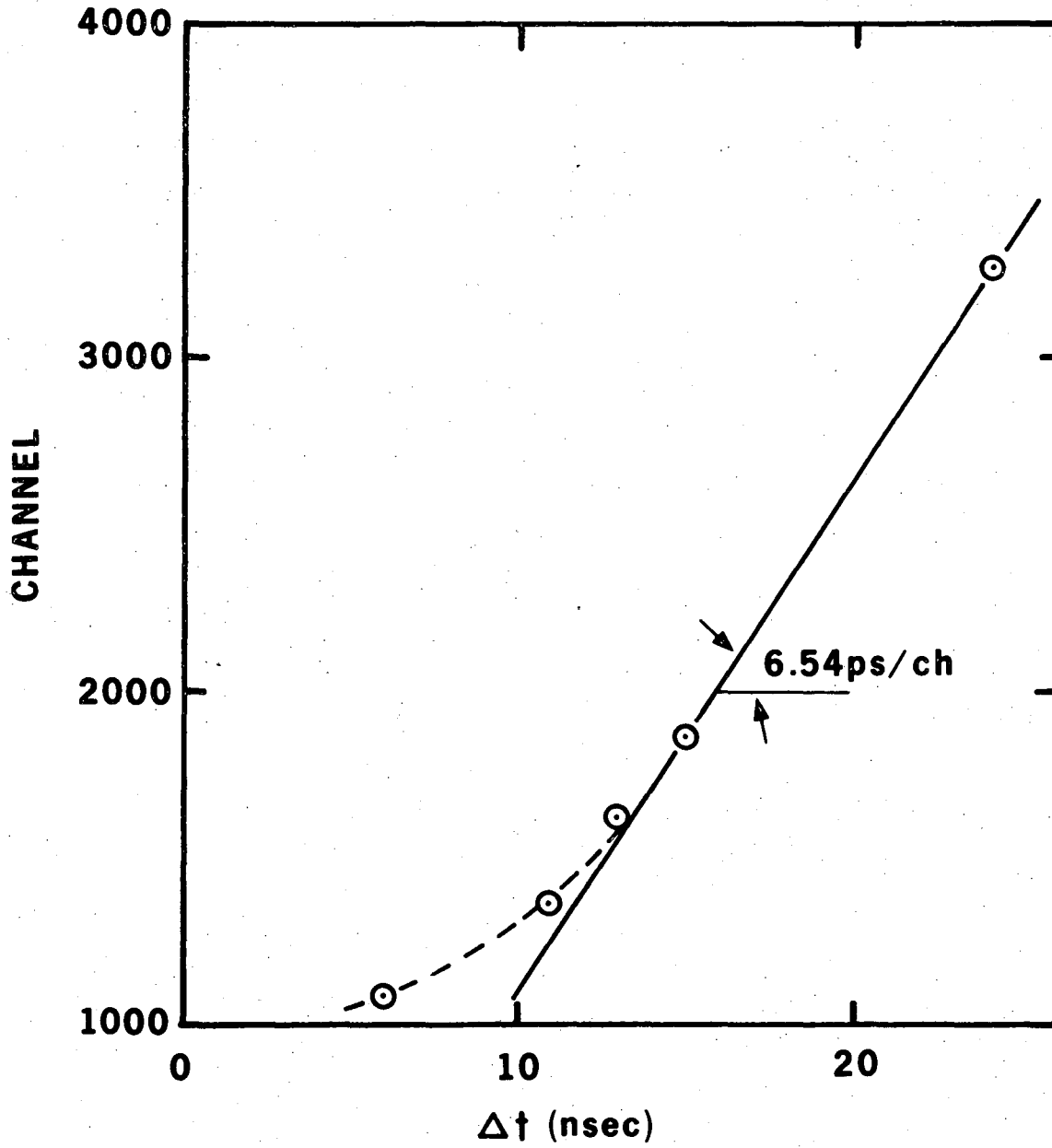
XBL755-4895

Fig. 6



XBL755-4896

Fig. 7



XBL 755-1382

Fig. 8

**LEGAL NOTICE**

*This report was prepared as an account of work sponsored by the United States Government. Neither the United States nor the United States Energy Research and Development Administration, nor any of their employees, nor any of their contractors, subcontractors, or their employees, makes any warranty, express or implied, or assumes any legal liability or responsibility for the accuracy, completeness or usefulness of any information, apparatus, product or process disclosed, or represents that its use would not infringe privately owned rights.*



TECHNICAL INFORMATION DIVISION  
LAWRENCE BERKELEY LABORATORY  
UNIVERSITY OF CALIFORNIA  
BERKELEY, CALIFORNIA 94720